Modern Environmental Science and Engineering (ISSN 2333-2581)
October 2018, Volume 4, No. 10, pp. 971-978
Doi: 10.15341/mese(2333-2581)/10.04.2018/007
Academic Star Publishing Company, 2018
www.academicstar.us

Change Detection in Multitemporal Remote Sensing Images Using Support Vector Machines and Pixel Relevance

Neide Pizzolato Angelo[1], and Rute Henrique da Silva Ferreira[2]

1. Federal University of Pelotas – UFPel, Brazil

2. La Salle University – UNILASALLE, Brazil

Abstract: This paper investigates an approach to the problem of change detection in multitemporal remote sensing images using Support Vector Machines (SVM) based on RBF kernel (Radial Basis Function) combined with a new relevance metric called Delta b (Δb). The methodology is based on the difference of the fraction images produced for each date. In images of natural scenes the difference in soil and vegetation fractions tends to have a symmetrical distribution around the mean of its pixels. This fact can be used to model two normal multivariate distributions: change and non-change. The Expectation-Maximization algorithm is implemented for estimating the parameters (mean vector, covariance matrix, and prior probability) associated with these two distributions. Random samples are extracted from these two distributions and used to train a SVM classifier based on RBF kernel. The proposed methodology is tested using multi-temporal data sets of multispectral images Landsat-TM covering the same scene, located in Roraima state, in two different dates. Test samples are obtained by the use of Change Vector Analysis (CVA) and used to validate the estimation method of relevance. It is expected that this methodology could be applied to detection of change for multispectral and hyperspectral multitemporal images used in remote sensing.

Key words: change detection, support vector machines, kernel-based methods, fraction images, Expectation-Maximization algorithm

1. Introduction

Detecting changes in a set of images of the same scene taken at different times is of general interest to a great number of applications in various areas of knowledge, such as video surveillance [1], biology and medicine [2]. Particularly in the area of remote sensing, the techniques of detecting changes in multitemporal images have been applied in agricultural, forest, urban, glacial and ocean monitoring, among others [3].

Two main approaches to the problem of change detection have been proposed in the literature for use in remote sensing: the supervised method and the unsupervised method [4].

Although the supervised method offers some advantages compared to the unsupervised method, such as defining the nature of the type of change that occurred, obtaining training samples is often a difficult and expensive task. Consequently, the use of unsupervised methods for changes detection is, at the operational level, more indicated and has been widely explored by researchers in the development of their work [3].

Among the various unsupervised methods of change detection proposed in the literature, the most widely used is the one known as Change Vector Analysis (CVA).

Corresponding author: Rute Henrique Da Silva Ferreira, Ph.D.; research areas/interests: pattern recognition, digital image processing and machine learning algorithms for remote sensing data analysis. E-mail: rute.ferreira@unilasalle.edu.br.

An interesting technique for the treatment of change detection is presented in [5] using the concept of mixture pixel. The mixture pixels phenomenon occurs when the same pixel comprises two or more distinct classes, called in this context endmembers. Thus it is possible to derive a new set of data with the so-called fractional images, which inform in each pixel the fraction occupied by each of the terrain components. This approach has two advantages: it allows a sub-pixel level analysis and eliminates the need for radiometric normalization of images acquired at different dates. Thus, the difference images are produced from the subtraction of components generated from the multispectral images.

In recent years, researchers have focused on the use of kernel-based classifiers in various application areas such as face recognition, text categorization, time series prediction, and handwriting recognition with good results.

Among these classifiers are the Support Vector Machines (SVM), the Kernel Principal Component Analysis (KPCA), the Kernel Fisher Discriminant (KFD) and others [6].

SVM is a very interesting method for dealing with the problem of classificating hyperspectral images since it works very efficiently with spaces of high dimensions, and it also handles noisy samples in a robust way and produces the function that defines the boundary of decision from a subset of training samples [7].

In this work the changes detection problem is approached considering that the distributions for the classes "change" and "non-change" presenting a normal multivariate distribution. Based on this assumption, the Expectation-Maximization (EM) algorithm [8] is used to estimate the statistical parameters of these distributions and thus to obtain training samples for the later classification stage using the SVM classifier, using the RBF kernel and, from the results of this classification, a new pixel relevance metric is obtained. In order to evaluate this methodology, two experiments were carried out: one with pre-selected test samples obtained from the translated CVA method [9] and another comparing the results obtained in this work with those of [3] for the same image.

2. Material and Methods

The changes detection process investigated in this work consists of the following steps: preprocessing (where the images are recorded and the fraction images are produced), data analysis (production of images), estimation of parameters of the probability density function of classes through the EM algorithm, production of the training samples and classification with SVM and determination of pixels relevance from the classification results [9].

The difference images are produced from the subtraction of the vegetation and soil components and of the fraction images generated from the multispectral images [5] and the method used to estimate these fractions of the mixing components (endmembers) of each image pixel is the Linear Spectral Mixture Model (MLME) [10].

The values found by the MLME should best represent the components (endmembers) for the image in question. The fractionation result will count with a number of images equal to the number of components chosen to represent the region.

In the images used in remote sensing, the vegetation, soil and shade/water components are frequently used. However, in this work only the vegetation and soil components were used, similarly to what was proposed in [3].

Fig. 1 shows the scattering of the difference image data, considering in the vertical axis the differences of soil fraction and in the horizontal the differences of vegetation fraction.

By analyzing Fig. 1, a negative correlation between the distribution of vegetation and soil fractions can be verified.

For this image it is expected that the pixels that have not undergone significant change between the two dates (non-change class) occupy a region near the center of the dispersion diagram (inserted in the circle of Fig. 1), whereas pixels that have undergone changes tend to dislocate to one of the two ends of the data dispersion diagram, depending on the type of change in these pixels (soil region changing to vegetation or vice versa) [9].

Classes ω_1 and ω_2, respectively, are considered here as the change and non-change classes. Thus, M_1, S_1, $P(\omega_1)$, M_2, S_2, $P(\omega_2)$ represent the averages vectors, covariance matrices and a priori probabilities of each class. For initial values of the parameters in the EM algorithm, some considerations are necessary and can be illustrated in Fig. 1.

The change class has a bivariate normal distribution, elongated in the direction of greater dispersion, which is estimated by the first eigenvalue (λ_1). Thus, for initial value in EM, using the covariance matrix for all samples of differences in fractions is suggested. The samples of the non-change class, however, are concentrated around the origin, presenting a small dispersion, caused by the inevitable noises in the data and non-significant changes present in this class. This dispersion will be estimated by the variance in the orthogonal direction to the one of greater variation (direction of the second eigenvector with magnitude estimated by the second eigenvalue - λ_2). The distribution of this class therefore tends to be in a circular region around the origin with a radius proportional to λ_2 [9].

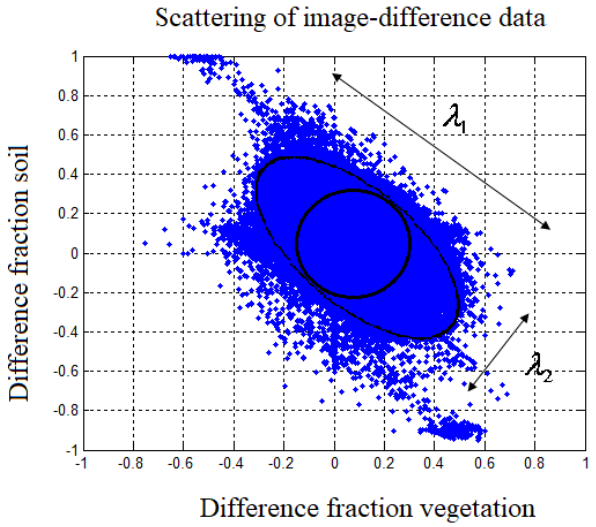

Fig. 1 Scattering of image-difference data [11].

Since the number of pixels exhibiting little change or no change is usually much greater than the number of those showing clear signs of change, the initial values of the a priori probabilities can initially be estimated to be 0.1 for change and 0.9 for non-change.

Thus, the initial estimates for each class that were used in the EM algorithm to obtain the parameters of the change and non-change classes are given by:

$$M_1 = \begin{bmatrix} 0 \\ 0 \end{bmatrix}, S_1 = \begin{bmatrix} \text{covariance matrix} \\ \text{of the} \\ \text{total sample} \end{bmatrix}, P(\varpi_1) = 0.1, \quad (1)$$
$$M_2 = \begin{bmatrix} 0 \\ 0 \end{bmatrix}, S_1 = \begin{bmatrix} \lambda_2 & 0 \\ 0 & \lambda_2 \end{bmatrix}, P(\varpi_1) = 0.9$$

After the application and convergence of the EM algorithm for these initial parameters, the estimated parameters of the change and non-change class distributions were generated and from these were generated the training samples that will be used to train the SVM classifier.

The SVM classifier, used in this work, is based on [12], whose problem can be expressed by equations (2) and (3).

$$\text{Maximize: } \sum_{i=1}^{M} \alpha_i - \frac{1}{2} \sum_{i,j=1}^{M} \alpha_i \alpha_j y_i y_j K(\mathbf{x}_i, \mathbf{x}_j) \quad (2)$$

$$\text{Subject to: } \sum_{i=1}^{M} \alpha_i y_i = 0 \text{ and } C \geq \alpha_i \geq 0 \text{ for } i = 1, \ldots, M \quad (3)$$

where: α are Lagrange multipliers, M is the number of samples considered, K ($\mathbf{x}_i$, $\mathbf{x}_j$) is the kernel function and C is the margin parameter or cost constant.

In this work the RBF kernel, described in equation (4), was used.

$$K(\mathbf{x}, \mathbf{x}') = e^{-\gamma \|\mathbf{x} - \mathbf{x}'\|^2} \quad (4)$$

The algorithms used to implement the SVM classifier were developed in the MATLAB software. For the purpose of training the classifier, we used

random samples provided by the function mvnrnd.m, from the MATLAB function library, using in each case the parameters estimated by EM of the respective class distribution. The sample pixels, after being generated by this function, are evaluated in the two functions of probability distributions for soil and vegetation, so that the sampled pixel that presents the highest probability of belonging to one of the distributions is labeled in the class corresponding to that distribution. By proceeding like this, we intend to ensure, statistically, that randomly generated samples represent, in fact, the classes they represent.

The RBF kernel SVM classifier is then trained with these samples, generating a decision function that will be used for class separation. Finally, from the results obtained by this decision function the metrics of estimation of pixel relevance are obtained, being from now on called Delta b (Δb).

The Δb metric is the vector resulting from the difference between the value of the decision function generated by the SVM classifier at any pixel of the image and the value of the decision function of the projection of this point on the optimal separation hyperplane in a direction parallel to the direction determined by the axis corresponding to the dependent variable of the decision function, as shown in Fig. 2 below. More details can be seen in [9].

Fig. 2 presents a view of the x_1x_3 plane of space R^3 (mapped or characteristic space), where a pixel $x_a = (x_1, x_2, x_3)$ is mapped from the original space (difference image) to this space. This point is inserted in a plane determined by the decision function $D(x_a) = b_a$ (plane in red), where b_a corresponds to the value of the decision function for the point x_a. This plane is parallel to the plane of optimal separation between the change and non-change classes, which is characterized by the decision function D(x) = 0 (gray plane). The projection of point a parallel to the axis x_3 on the plane of optimal separation determines point x_a'. The difference between the values of the decision function for these points defines the vector Δb. The angle determined between this vector and the vector normal to the optimal separation hyperplane (vector w) is β.

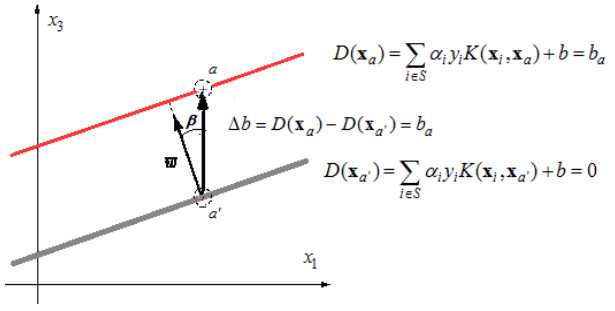

Fig. 2 Visualization of the relevance metric Δb.

It should be emphasized that this metric does not estimate a percentage change value of the pixel over time, nor even has a specific statistical significance, but estimates the degree of confidence with which a pixel can be labeled in a particular class. Considering that there are only two complementary classes in change detection (change and non-change), one can use only the relevance on one of them, in this case, the one that refers to the change classes, because it is possible to declare that a pixel having high relevance in one of the classes means that it has low relevance in the other and vice versa. Thus, this metric will allow the estimation of a pixel relevance classified to the class change only by the value of Δb. The relevance value represented by $P_c(x)$ for the change class will be given by the ratio between the highest value of Δb and the smallest value of Δb, according to Eq. (5), as follows:

$$P_c(\mathbf{x}) = \begin{cases} \dfrac{\Delta b}{\max(\Delta b)}, & \text{if } \Delta b > 0 \\ 0.5, & \text{if } \Delta b = 0 \\ 1 - \dfrac{\Delta b}{\min(\Delta b)}, & \text{if } \Delta b < 0 \end{cases} \tag{5}$$

and the relevance of the non-change class $P_{nc}(\mathbf{x})$ is given by equation (6):

$$P_{nc}(\mathbf{x}) = 1 - P_c(\mathbf{x}) \tag{6}$$

It can be seen from the above equations that the lowest value of Δb obtained after the classification will correspond to 0 (0% of relevance to the class) and the

largest value of Δb will correspond to 1 (100% relevance to the class), that is, pixels with values of Δb zero, or close to zero, indicate that they are unlikely to belong to the change class and therefore have a high probability of belonging to the non-change class. Similarly, pixels with value 1 or close to 1 will indicate a high probability of belonging to the change class and, therefore, low probability of belonging to the non-change class.

At this point, it is necessary to state that the determination of this relevance metric is dependent on the choice of the kernel used and the parameters assigned to it during the classification process with SVM.

3. Results and Discussion

Two Landsat 5-TM images covering the same area were considered for the experiment, located in the state of Roraima, as shown in Fig. 3. The image of the first date was acquired in October 1991 and the image of the second date in April 1994. In the experiments, only the resulting fractions for vegetation and soil were considered. The images used have 390.625 pixels distributed in a square of 625 by 625 pixels.

(a)

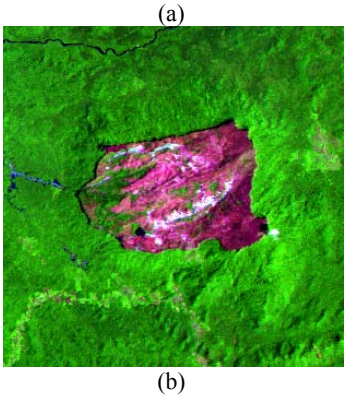

(b)

Fig. 3 (a) Image of Date 1, composition in false color 5 (R), 4 (G), 3 (B). (b) Image of Date 2, composition in false color 5 (R), 4 (G), 3 (B).

Two procedures were used to evaluate the accuracy of the results in this study:

a) Quantitative analysis carried out through the production of a set of controlled test samples using the adapted Change Vector Analysis (CVA) technique. [9].

b) Qualitative and quantitative analysis carried out through the construction of a map of relevance for the whole image.

For the quantitative evaluation, we used a set of randomly collected test samples from the fraction difference image with the vector change module recommended in the CVA technique, however, instead of considering the origin of the change vectors in (0.0) the origin of the vectors translated to the mean of the non-change class was considered. The test samples were taken like this because no terrestrial truth data were available for the study image. The translated CVA technique [9] will generate for each image pixel a vector having as its origin the data of the image pixel taken at date 1, and as the end of that vector the data of the same pixel taken at date 2, both considering as the origin of the vector system the mean of the non-change class. The use of this technique will allow a reliable estimation of the change in the sampled pixels, that is to say, pixels presenting a translated CVA module with values greater than 0.3 and lower than 0.6 will correspond to pixels that showed some significant change over the period. Module values above 0.6 were disregarded so that no corresponding shade and cloud samples were used, which certainly corresponded to the change, but did not represent the soil and vegetation components. Pixels with transferred CVA module smaller than 0.1 are those that did not show significant change over the period. The choice of these intervals is to ensure that the test samples are representative of their respective classes.

Thus, with the use of the transferred CVA module, 900 pixels of sample were collected for each class, in a random and uniform way throughout the difference image, guaranteeing samples with comprehensiveness throughout the image and without any bias in their choice. The samples thus collected should be used to statistically prove the efficiency of the method for determining relevance.

Table 1 shows, in order, the best and worst result for each training sample set used in the RBF kernel SVM classifier for the following variables: the mean of the relevance value, the standard deviation of the relevances, and finally, the percentage of pixels correctly classified in the change and non-change classes.

Table 1 Evaluation of relevance in the test sample generated from the CVA Module with translated center and using RBF kernel for change and non-change classes.

Number of training samples for the classifier	Kernel coefficient (γ)	Average relevance value in the change class (%)	Standard deviation of relevance in the change class (%)	Percentage of pixels classified with relevance above 50% in the change class	Average relevance value in the non-changing class (%)	Average relevance value in the non-changing class (%)	Percentage of pixels classified with relevance above 50% in the non-change class
200	1	65.96	9.36	100.00	87.70	9.58	100.00
200	2	65.58	9.50	100.00	74.31	15.16	87.56
300	1	67.67	10.33	100.00	90.00	9.24	100.00
300	95	69.43	9.63	100.00	84.55	11.23	99.67

From the results presented in the table above for the relevance obtained with the RBF kernel, it is observed that with the appropriate parameters, the pixels of the test sample were correctly classified according to the relevance informed by the metric Δb, showing a minimum hit above 87% of pixels, in the worst case. Thus, the results, generally speaking, show that the proposed metric can adequately classify the pixels of the test sample in the change and non-change classes, according to the distributions theorized for them. Based on the good relevance results obtained with the test sample, one can affirm that the relevance metric Δb is efficient.

For the second experiment, a qualitative and quantitative analysis of the study image was performed using 200 and 300 training samples for each class and for the parameter γ the values 5, 10, 80, 85, 90, 95 and 100, where the results were compared to those obtained in [11]. This comparison aims to corroborate the quality of the proposed metric in relation to another already accepted in the literature, due to the lack of terrestrial truth data of the image in use.

Fig. 4 shows in (a) and in the map of difference between the relevance of the methodology proposed and that used in [11] and in (b) the map of relevance to the proposed methodology using the RBF kernel with 300 training samples and $\gamma = 90$.

A qualitative analysis by means of a visual inspection on the map of Figure 4a) shows that the relevance map generated by the proposed methodology and the one obtained in [11] are very similar, since the difference between these relevances in most pixels ranges from -0.15 to 0.15. In Fig. 4b) the pixel relevance map using RBF kernel SVM for 300 training samples and $\gamma = 90$ is presented, which has the best correlation between the relevance values in the two methodologies. The value of the Person correlation coefficient R calculated between these maps presents an expressive value ($R = 0.9728$) which characterizes a highly significant correlation between them. In addition, the mean differences between maps are close to -0.0176, with a standard deviation of approximately 0.092. It was also found that the R value calculated over all the tests in this experiment for various sample sizes and values γ, except for the test with 200 training samples and $\gamma = 5$ (with $R = 0.66$), had an R coefficient higher than 0.80. Thus, except for one test, all the

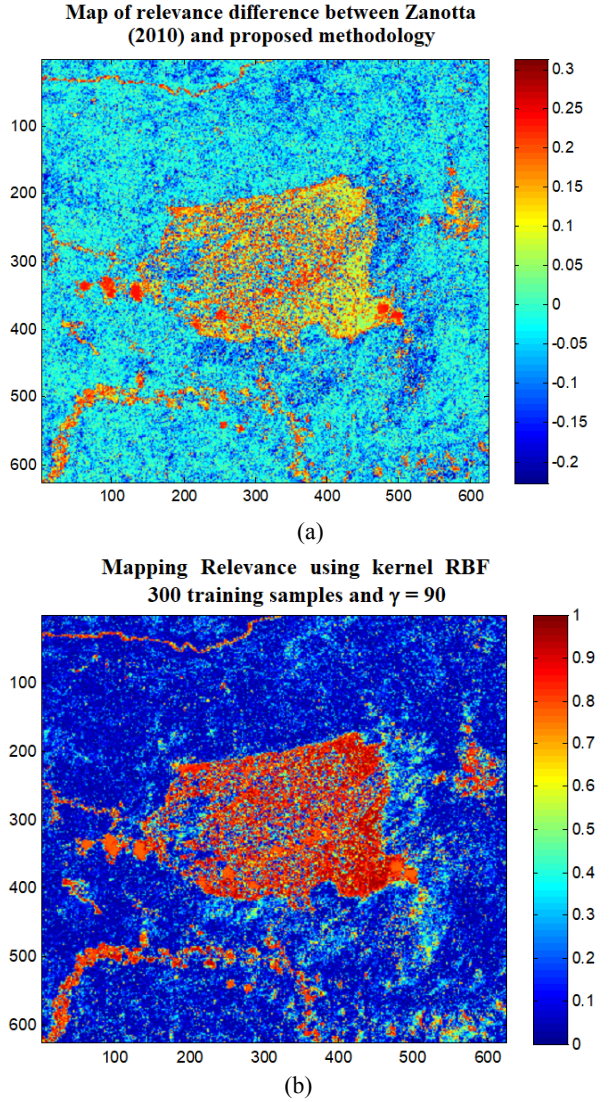

Fig. 4 a) Map of relevance difference between Zanotta (2010) and proposed methodology. b) Mapping Relevance using kernel RBF 300 training samples and γ = 90.

others present a very significant correlation between the relevance maps.

Thus, the measures of pixel relevance proposed in this work are highly correlated to the relevance measure presented in [11].

4. Conclusion

The experiments developed in this work show the adequacy of the proposed methodology, producing results that are quite acceptable in the detection of changes in soil cover. In particular, in the experiment involving all the pixels of the image under study, the pixel relevance results obtained in this work are similar to those obtained in [11].

However, despite these good results, it is important to point out that the proposed method is aimed at detecting changes in environments where vegetation and soil components prevail. Therefore, it is not possible to affirm that this methodology, when applied to images with different components, presents results similar to those obtained in this work.

However, since the results are compatible with those of Ref. [11] and they were obtained with few training samples, one of the characteristics of the SVM classifier, it is expected that this relevance metric can be applied in the detection of change in multispectral images, both multispectral and hyperspectral images in remote sensing. In particular, in the latter, with better results, since the SVM classifier is not to be affected by the Hughes phenomenon, unlike parametric classifiers like the one used in [11].

Acknowledgment:

The authors would like to thank Professor Vitor Haertel (in memoriam) for the fundamental role he played in their academic trajectories.

References

[1] Xiaogang Wang, Meng Wang and Wei Li, Scene-specific pedestrian detection for static video surveillance, *IEEE Transactions on Pattern Analysis and Machine Intelligence* 36 (2014) (2) 361-374.

[2] M. Bosc, F. Heitz, J. P. Armspach, I. Namer, D. Gounot and L. Rumbach, Automatic change detection in multimodal serial MRI: Application to multiple sclerosis lesion evolution, *Neuroimage* 20 (2003) (4) 643-656.

[3] D. Zanotta and V. Haertel, Gradual land cover change detection based on multitemporal fraction images, *Pattern Recognition* 45 (2012) (1) 2927-2937.

[4] L. Bruzzone, R. Cossu and G. Vernazza, Detection of land-cover transitions by combining multidate classifiers, *Pattern Recogniton Letters* 25 (2004) (13) 1491-1500.

[5] V. Haertel, Y. E. Shimabukuro and R. Almeida Filho, Fraction images in multitemporal change detection, *International Journal of Remote Sensing* 10 (2004) (23) 5473-5489.

[6] J. Shawe-Taylor and N. Cristianini, *Kernel Methods for Pattern Analysis*, Cambridge University Press, UK, 2004, p. 477.

[7] Camps-Valls and G. Bruzzone, L. Kernel-based methods for hyperspectral image classification, *IEEE Transactions on Geoscience and Remote Sensing* 43 (2005) (6) 1351-1362.

[8] R. O. Duda, P. E. Hart and D. G. Stork, *D. G. Pattern Classification* (2nd ed.), New York: John Wiley & Sons, 2001, p. 680.

[9] N. P. Angelo, Uma Abordagem para a Detecção de Mudanças em Imagens Multitemporais de Sensoriamento Remoto Empregando Support Vector Machines com uma Nova Métrica de Pertinência, 2014, p. 125, Tese (Doutorado em Sensoriamento Remoto), UFRGS, Porto Alegre.

[10] Y. E. Shimabukuro and J. A. Smith, The least-squares mixing models to generate fraction images derived from remote sensing multispectral data, *IEEE Transactions on Geoscience and Remote Sensing* 29 (1991) (1) 16-20.

[11] D. Zanotta, Uma Abordagem Fuzzy na Detecção Automática de Mudanças do uso do Solo Usando Imagens de Fração e Informações de Contexto Espacial, 2010, p. 87, Dissertação (Mestrado em Sensoriamento Remoto), UFRGS, Porto Alegre.

[12] S. Abe, *Support Vector Machines for Pattern Classifications*, Kobe, Japão: Ed. Springer, 2005, p. 343.